Conceptual Studies of Combined-Cycle Engine

Takeshi Kanda
Japan Aerospace Exploration Agency, Space Propulsion Research Center
1 Koganesawa, Kimigaya, Kakuda, Miyagi 981-1525, Japan
kanda.takeshi@jaxa.jp

Keywords: Combine-cycle engine, SSTO, Conceptual study

Abstract

Conceptual studies of a combined-cycle engine have been conducted. Herein, the results are presented. The engine is composed of ejector-jet, ramjet, scramjet and rocket modes, and will be mounted on the Single-Stage-to-Orbit aerospace plane. Propellants are hydrogen and oxygen. Calculated engine thrust performances and cooling requirement of the engine are presented. Pitching moment of the plane with the engine will be balanced even in the vacuum condition. The experimental results of the inlet and the ejector-jet, ramjet and scramjet modes are presented. The effect of the airframe configuration on the engine performance and the thermal environment in the inside of the plane are also presented. Through the investigations, possibilities of the combined-cycle engine and the aerospace plane are being made clear now.

Introduction

Studies of the aerospace plane have been conducted. Figure 1 shows an artist image of the plane. Several kinds of engines or operating modes are necessary to go to an orbit. There are two engine systems for this requirement; the combined-cycle engine system and the combination engine system. The combined-cycle engine has several operating modes in a single engine. Several kinds of such engines have been proposed and studied.[1-4] In the combination engine system, several engines are mounted on a vehicle.[5] Each engine of the system will have performance higher than that of the combined cycle engine. However, during operation of one engine, additional engines may add drag, and they will add deadweight when turned off. Although the combined cycle engine will show lower performance at each operating mode, it will be lighter and will not induce additional drag.

Fig. 1 Image of SSTO aerospace plane.

Conceptual studies of the combined-cycle engine have been conducted in the engine system team of the Japan Aerospace Exploration Agency, formerly the National Aerospace Laboratory of Japan. The engine is suitable to the Single-Stage-to-Orbit (SSTO) aerospace plane and composed of ejector-jet, ramjet, scramjet and rocket modes. Experimental component studies have been also conducted to evaluate the

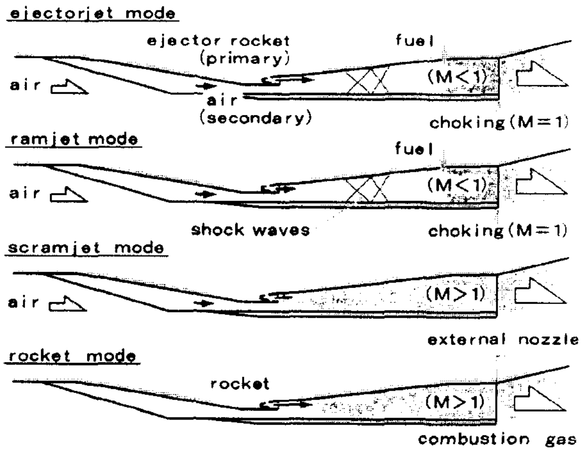

Fig. 2 Operating conditions of the combined-cycle engine.

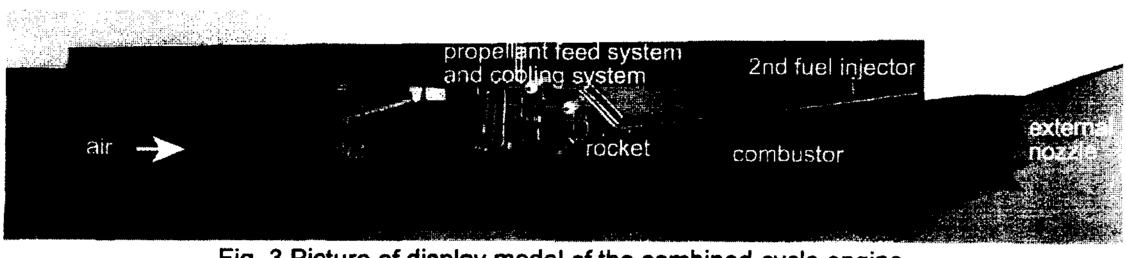

Fig. 3 Picture of display model of the combined-cycle engine.

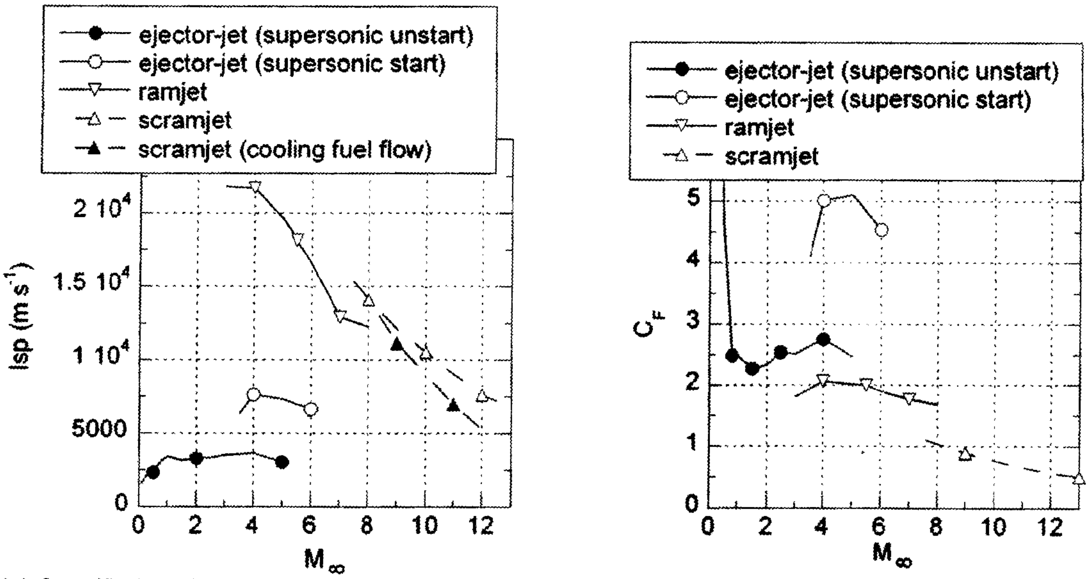

(a) Specific impulse (b) Thrust coefficient

Fig. 4 Engine thrust performance.

models in the conceptual studies and to model the physical phenomena in the engine for the conceptual studies. Herein, results of the studies are presented.

Combined-Cycle Engine

Figure 2 shows a schematic diagram of the engine operating conditions. From take-off to about Mach 3, the engine works as an ejector-jet, that is, an air-breathing rocket, or an ejector ramjet. The rocket works as an ejector-rocket. The breathed air and the rocket exhaust decelerated to subsonic speed. Fuel is injected and the combustion gas chokes at the engine exit. Secondary fuel injection and subsonic combustion attained higher mixing and combustion efficiencies.[6] From Mach 3 to 7, the engine works as a ramjet. The rocket works as an ignitor. From Mach 7 to 11, the engine works as a scramjet. The rocket supplies fuel-rich pre-combustion gas as fuel. From Mach 11, the space plane goes to space.

The engine has a fixed geometry. Only the inlet ramp is movable and closes the engine entrance in entry flight from space to the earth, as described later.[7] Adoption of movable engine configuration will be difficult. In the movable engine, the rocket section cooled with liquid hydrogen will have to move with the other components. The protect gas from gaps between the wall panels will reduce impulse function. Shortening or extension of the movable panels will be also a problem.

Small number of rocket engines is mounted in the engine, due to simplicity of the engine and avoidance of difficulty in development. Each rocket becomes large, and should be mounted on the top wall, where plumbing of the rockets to the propellant tanks and turbo-pumps is easy. Figure 3 shows a picture of a display model of the combined-cycle engine. In the display model, four rockets are mounted in each module. In the ejector-jet and the ramjet modes, the subsonic combustion gas chokes at the exit of the engine with no geometrical throat.

Studies of Engine System

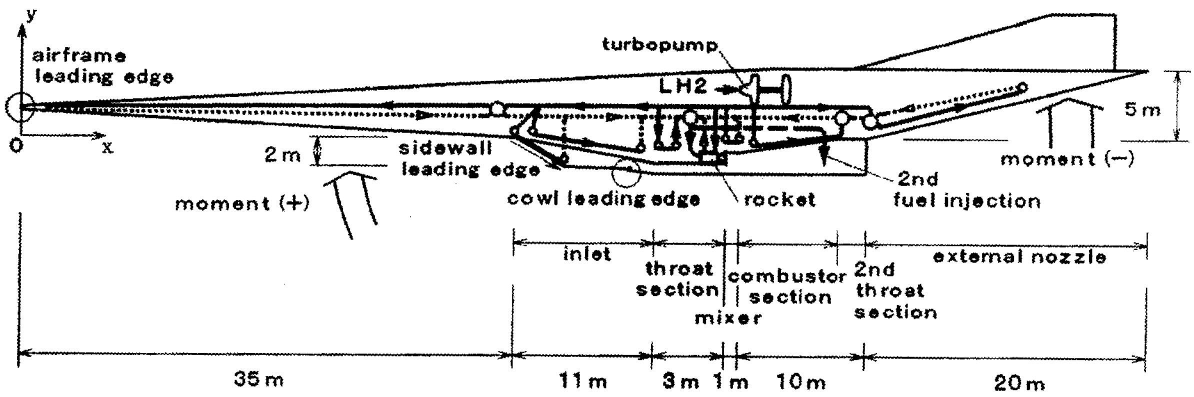

Fig. 5 Cooling system diagram and direction of pitching moment.

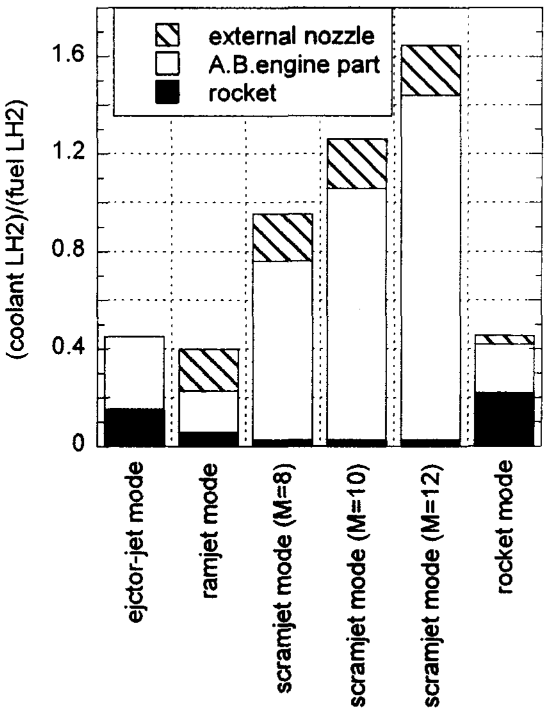

Fig. 6 Cooling requirement.

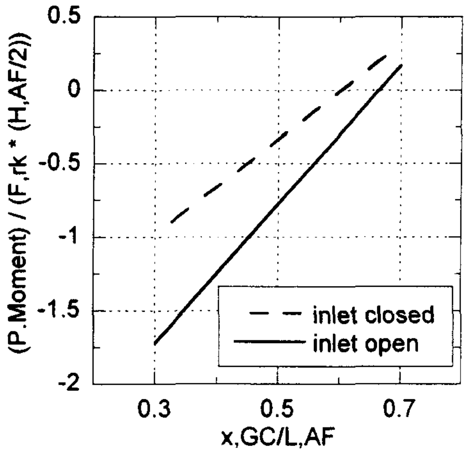

Fig.7 Effect of gravity center on pitching moment of SSTO plane.

Thrust performance and cooling requirement

Figures 4(a) and (b) show the specific impulse and the thrust coefficient of the engine.[8] There were three operating conditions around Mach 4; the ejector-jet mode under the inlet-unstarted condition, the ejector-jet mode under the inlet-started condition and the ramjet mode. In the scramjet engine, cooling requirement became larger than the stoichiometric fuel flow rate.[9] In the combined-cycle engine, cooling of the rockets is further required. The requirement of the combined-cycle engine might be further increased.

With the calculated gas flow conditions, cooling requirement was calculated.[8] Figure 5 shows a schematic diagram of the regenerative cooling system of the engine and a part of the airframe. The leading edge and the external nozzle were cooled with a silicone fluid. Figure 6 shows the cooling requirements. In the scramjet mode, the pressure and temperature in the combustion chamber of the rocket were not high.

So the cooling requirement in the scramjet mode was near the requirement of the pure scramjet. But, the requirement became larger than the stoichiometric fuel flow rate. According to flight simulation, the operation of the scramjet mode was effective until Mach 11.

Pitching moment of SSTO Plane

The combined-cycle engine will be mounted on windward surface of the plane to take compressed air by the airframe. But, the center of gravity will not locate on the thrust line of the engine. During the flight in air, aerodynamic control devices are effective to cancel the pitching moment. In a low flight dynamic pressure condition or in space, such devices are not effective anymore. Balance of the pitching moment of the SSTO plane was investigated in the vacuum condition.[8] The position of the gravity center is picked up as a parameter. The reference position of the gravity center is shown in Fig. 5. Fig. 7 shows the calculated results. The pitching moment was around 0. The large external nozzle of the rear windward surface of the airframe produced large negative pitching moment, and it balanced with the moment by the rockets. Even in vacuum condition, with such configuration of the space plane, the pitching moment of the SSTO plane will be balanced.

Thermal protection of engine in entry flight

The combined-cycle engine for SSTO plane has been studied. The thermal protection in the entry flight is also a problem to be discussed, as well as the protection in ascending flight. The cooling requirement of the engine was calculated with flight simulation.[7] Figure 8 shows the flight condition from a low earth

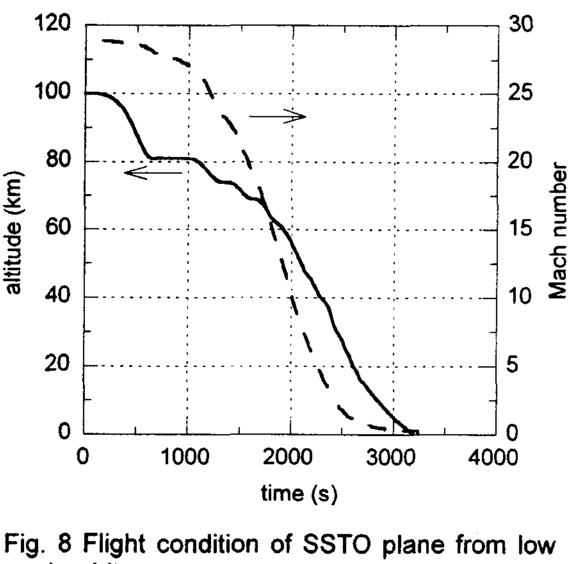

Fig. 8 Flight condition of SSTO plane from low earth orbit.

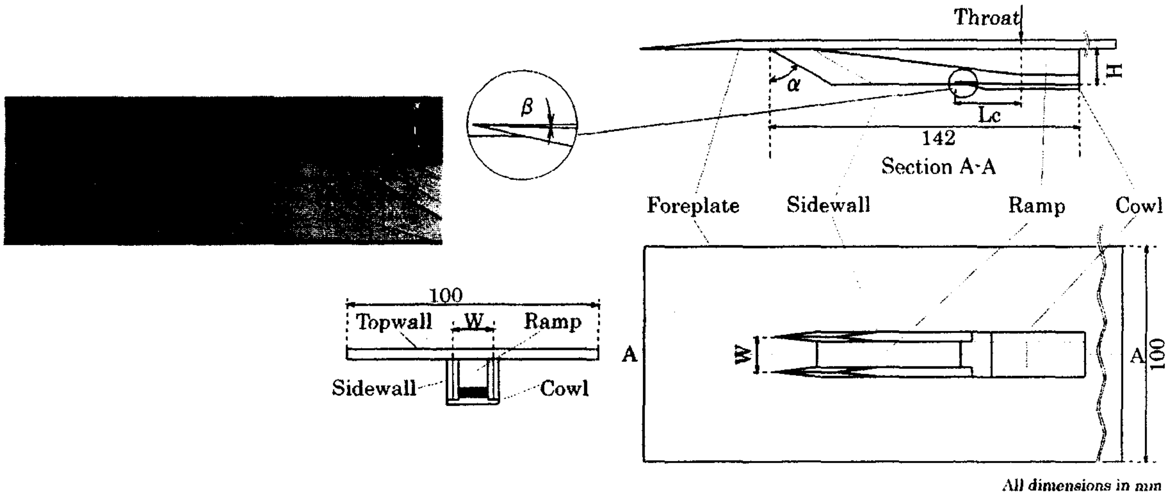

Fig. 9 Inlet model with drooped cowl.

orbit of 100 km. The simulation was conducted on two-dimensional plane. The SSTO plane was a material point. In the study, two engine configurations were investigated, i.e., the closed-inlet configuration and the open-inlet configuration. Under the open-inlet configuration, the inside of the engine was cooled regeneratively, as well as in the ascending flight. In the closed-inlet condition, the outer surface of the ramp panel of the inlet closed the engine, and only the ramp panel was cooled. According to the simulation, required amount of the coolant for the leading edge of the cowl was large in the open-inlet configuration. Additional weight of the movable mechanism of the inlet ramp and the protection gas from the gaps between the wall panels will be smaller than the amount of the required coolant in the open-inlet configuration. Herein, the closed-inlet configuration was adopted in the engine.

Experimental Studies

Tests of ramp compression inlet

The inlet of the combined-cycle engine will have to be closed in the entry flight to reduce amount of the coolant. Therefore, the inlet will be movable, and the inlet will be ramp-compression type. Though the sidewall-compression type inlet has been studied for the scramjet,[10,11] the study of the ramp-compression inlet is not sufficiently conducted in the system team. Furthermore, the combined-cycle engine will operate in broader flight region than the scramjet. High performance in the wider range is required to the inlet of the combined-cycle engine. Under the supersonic flight, the starting condition of the inlet in lower Mach numbers attains wider operating range of the ramjet mode of the engine. The aerodynamic performances and the starting ability of the ramp-compression type inlet has been investigated experimentally.[12] Figure 9 shows an inlet model and a schlieren picture of the model in Mach 4 airflow. The start ability was improved with the drooped cowl. It mitigated pressure increase and Kantrowitz-Donaldson criteria. The inlet also operates in subsonic and transonic airflow conditions. Characteristics of the inlet of the combined-cycle engine are now investigated.

Effect of sides-spillage

The engine modules will be mounted on the windward surface of the aerospace plane, as shown in Fig. 1. The airflow condition to the engine on the sides of the plane is different from the condition at the center of the plane. The effect of the sides-spillage from the airframe on the engine performance was investigated.[13] The mass capture and the total pressure performances of the inlet were investigated experimentally, then the one-dimensional calculation of the engine and the flight simulation were conducted.

On the sides, the mass flow rate was reduced, and the engine thrust decreased (Fig. 10). The sides-spillage reduced payload. The effect should be included in design of the engine and the SSTO plane.

Effect of integration of engine into airframe

The scramjet engine and the combined-cycle en-

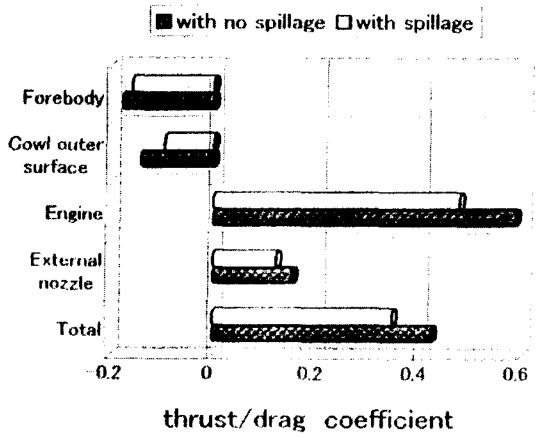

Fig. 10 Thrust/drag contents of the aerospace plane at a flight Mach number of 10.

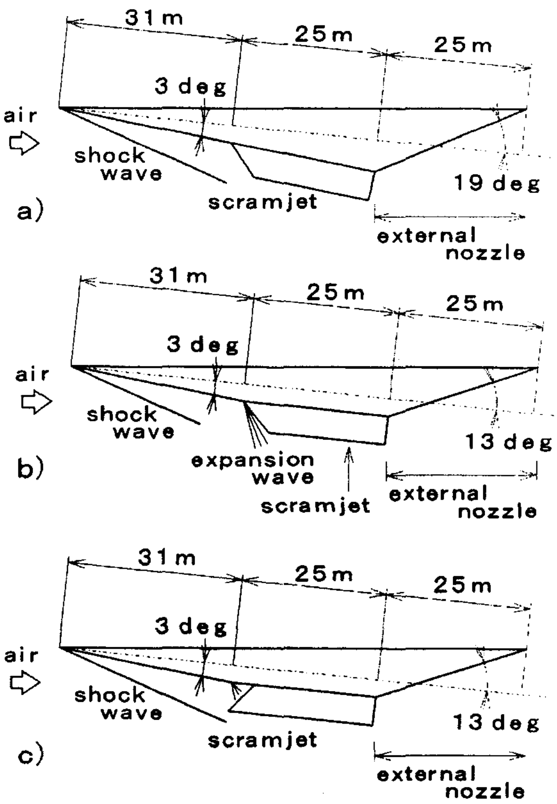

Fig. 11 Vehicle configuration models for performance calculation: a) engine integrated on the ramp of the airframe; b) engine attached downstream of the rear corner of the airframe ramp; c) inlet is located on the ramp and the rest of the engine parallel to the airframe axis.

engine will be integrated to the airframe, as shown in Fig. 1. Several types of airframe-engine integration have been proposed and schematically illustrated. The effect of the integration of the engine into the airframe on engine performances was investigated.[14] Several types of inlet-airframe models were examined experimentally, then the engine performances was calculated, and the flight simulation was conducted.

When the engine was attached downstream of the rear corner of the airframe-ramp, as shown in Fig, 1 b, the effect of the pre-compression due to the airframe disappeared, and the mass flow rate to the engine decreased. The inlet should be mounted on the ramp of the windward surface as in Figs. 11 a and c, and the rest of the engine should be parallel to the airframe axis to utilize the core thrust and the thrust due to the external nozzle.

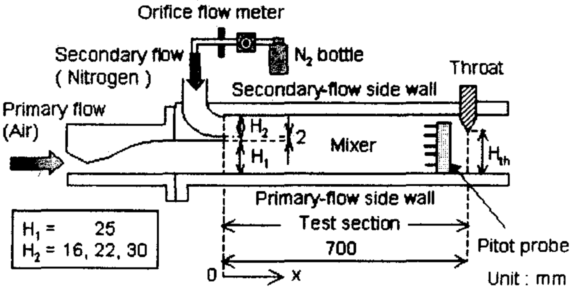

Fig. 12 Schematic diagram of ejector-jet test model.

Aerodynamic tests of ejector-jet

Suction, mixing and the pressure increase performances of the ejector-jet were tested experimentally to evaluate simple design models on the suction performance and the pressure increase performance.[15]

Fig. 13 Schlieren photograph around entrance of the test section in the ejector-jet test.

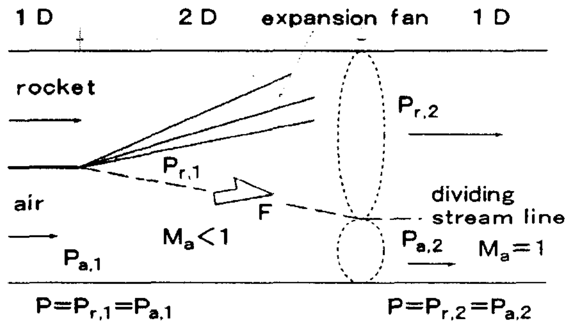

Fig. 14 Schematic diagram of a model for suction under aerodynamic choking.

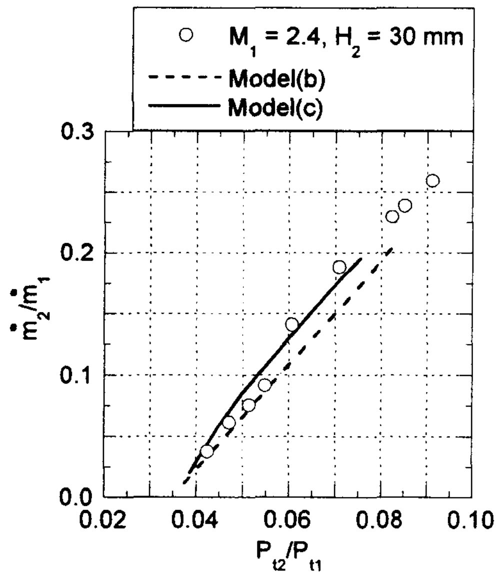

Fig. 15 Suction performance under the aerodynamic choking condition.

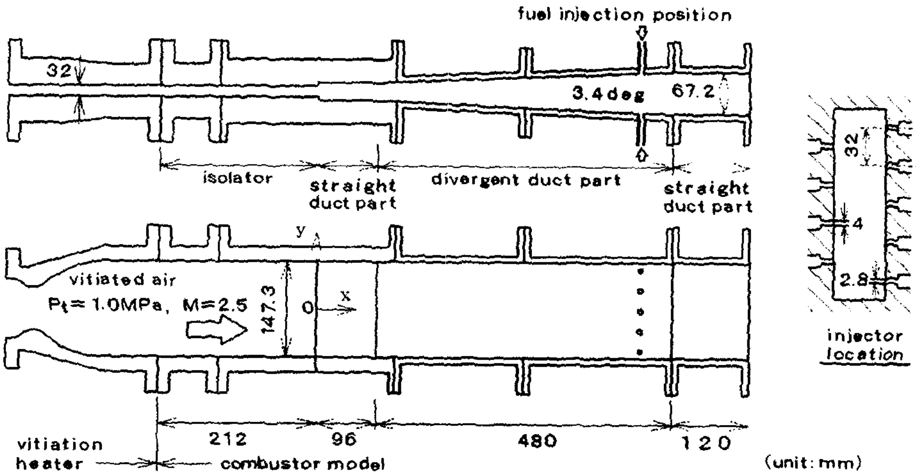

Fig. 16 Combustor model for dual-mode operation tests.

Figure 12 shows a schematic diagram of the test model. The rocket exhaust was simulated with M2.3 air. And the air in the actual engine was simulated with nitrogen. There was throttling valve downstream of the test section to simulate subsonic combustion and subsequent choking. Figure 13 shows a schlieren picture around the entrance of the test section. Figure 14 shows a schematic diagram of a model for suction under the aerodynamic choking.[8] In the aerodynamic choking condition, subsonic secondary flow chokes through the interaction with the primary flow.

Figure 15 shows suction performance and the model calculation results under the aerodynamic choking condition. The calculated results agreed well with the experimental results. The models will be used to design the engine.

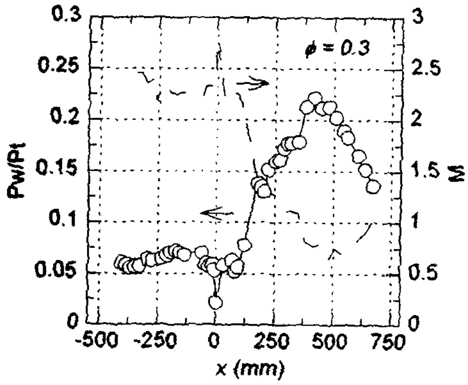

Fig. 17 Wall pressure and Mach number distributions under the downstream-combustion ramjet mode.

Combustion tests of ramjet mode

When the hydrogen fuel was injected in the downstream duct, as shown in Fig. 16, the downstream-combustion ramjet mode was attained.[16,17] Figure 17 shows distributions of wall pressure and Mach number under the total temperature of air of 800 K and the equivalence ratio of 0.3. The Mach number was calculated with the measured wall pressure. Air was decelerated in the divergent section, and the subsonic combustion gas choked at the exit of the model with no geometrical throat. The mode is different from the ordinary ramjet mode, in which air is decelerated in the isolator, and subsonic combustion gas chokes at the exit of the throat section of the combustor.

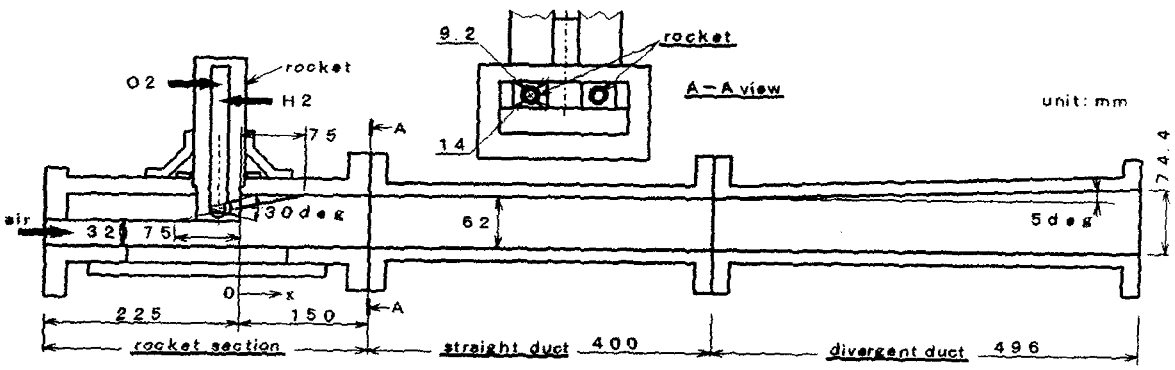

Fig. 18 Model of combined-cycle engine combustor.

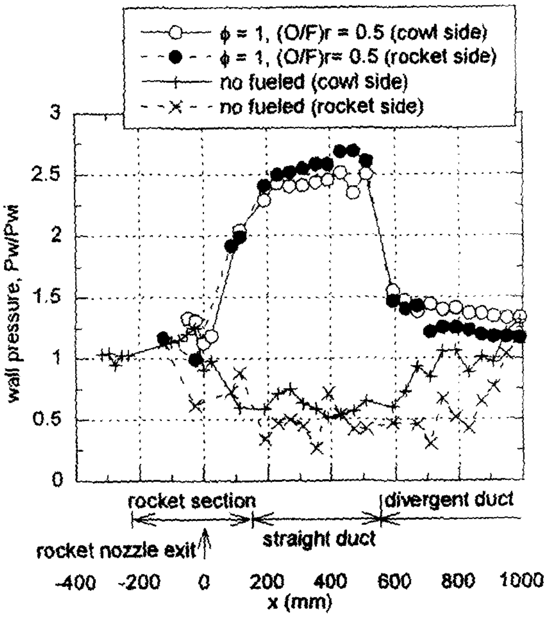

Fig. 19 Wall pressure distributions of the combined-cycle engine combustor under scramjet mode.

In the downstream-combustion ramjet mode, thrust performance will be lower than that of the ordinary ramjet mode. However, a long isolator will not be required. This combustion condition can be applied to the subsonic-combustion ejector-jet mode, where movable secondary throat is not required at the exit of the combustor. This experimental result is adopted in the combined-cycle engine.

Combustion tests of scramjet mode

In the combined-cycle engine, fuel-rich, pre-combustion gas is supplied from the rockets as fuel. The injector geometry of the rockets is different from those of the conventional scramjet injectors. Furthermore, the gas is injected parallel to the airflow from the inlet. Mixing and combustion in the scramjet engine is a key issue. The combustion tests should be conducted and be certificated operability of the combustor in the early stage of the combined-cycle engine research.

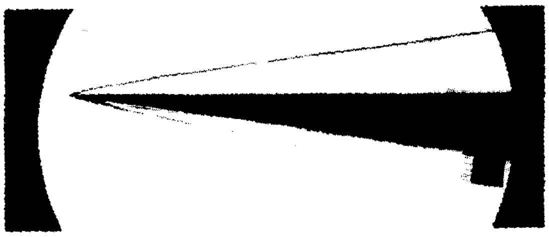

Fig. 21 Schlieren picture of the forebody model in Mach 10 airflow.

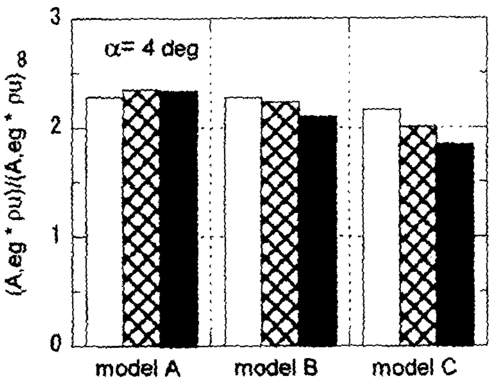

Fig. 22 Airflow rate into the engine in Mach 10 flow.

Figure 18 shows the combustor model of the combined-cycle engine and it was tested under the total temperature of 2400 K and Mach number of 2.4 of the inflow vitiated air, i.e., under the scramjet mode condition.[18] Propellants were hydrogen and oxygen. Figure 19 shows the wall pressure distributions. The mixture ratio in the rocket, O/F, was 0.5 and the equivalence ratio for the airflow was 1. Measured combustion efficiency was 0.8 at the exit of the combustor. Sufficient combustion was attained with such a rocket fuel injector of the combined-cycle engine.

Effect of airframe configuration on airflow to engine

The combined-cycle engine will be mounted on the windward surface of the aerospace plane, and the fore-body of the airframe works as the external inlet

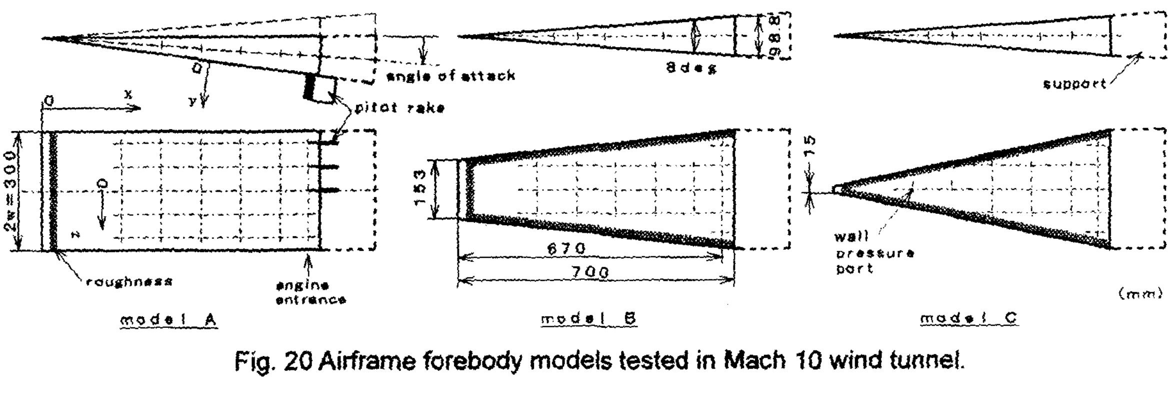

Fig. 20 Airframe forebody models tested in Mach 10 wind tunnel.

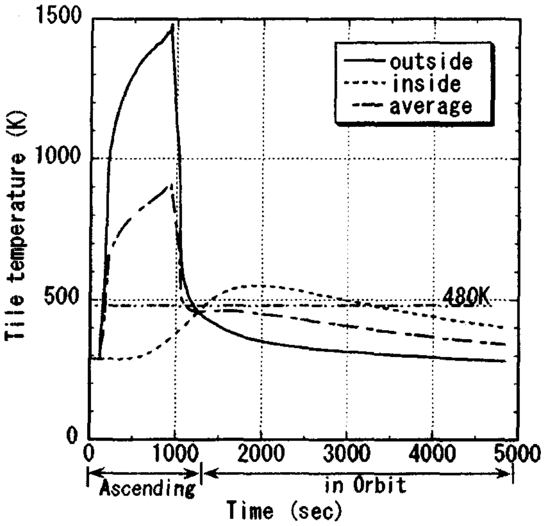

Fig. 23 History of tile temperatures in ascending flight.

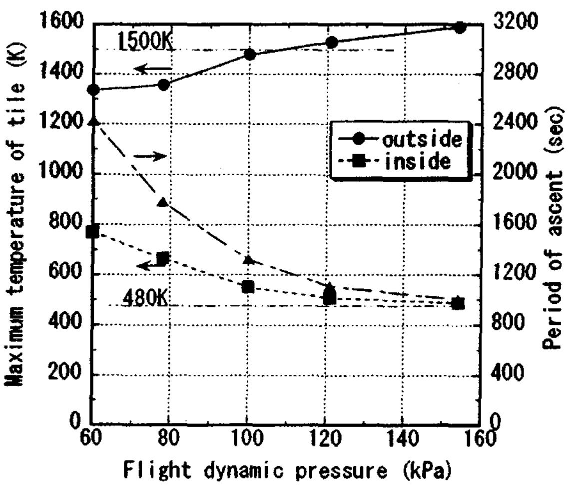

Fig. 24 Maximum temperature during ascending flight against flight dynamic pressure.

in the supersonic and hypersonic flight. The airframe configuration of the aerospace plane affects the airflow condition to the engine. The effect was investigated numerically[19] and tested in Mach 10 wind tunnel.[20] Figure 20 shows a schematic diagram of the forebody models of the aerospace plane airframe. The model A had a line leading edge, and the model B had an edge with half length of the body width. The model C had a narrow leading edge.

Figure 21 shows a schlieren picture of the model A in the test. Figure 22 shows airflow rates to the engine of the three models. The rates were normalized with mass flux of the core flow of the wind tunnel and the projected area at the imaginary engine entrance. The airflow rate into the engine was large in the model with long leading edge. The forebody configuration with the line leading edge is suitable to increase the engine thrust.

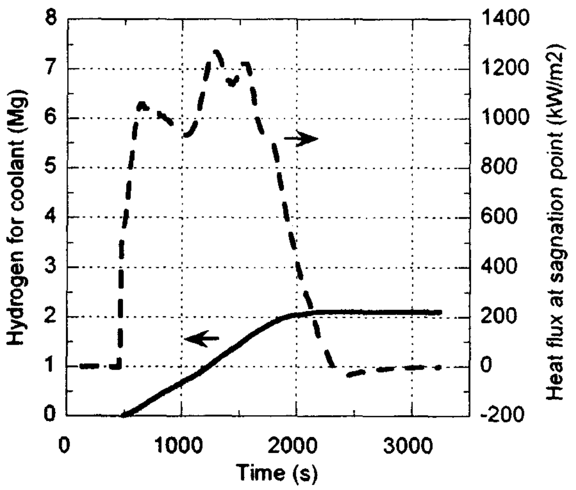

Fig. 25 Hydrogen coolant mass.

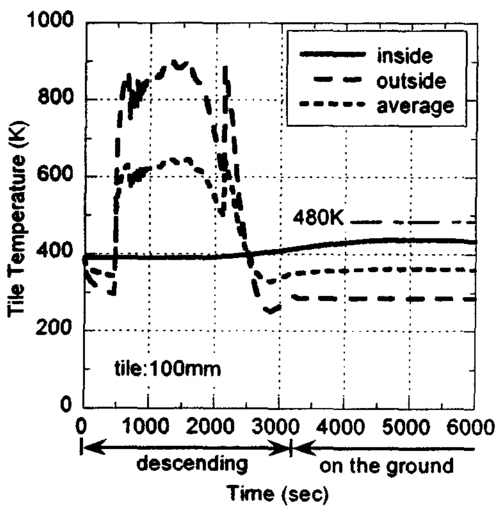

Fig. 26 History of tile temperatures.

When the airframe has geometry like the model C, the boundary layer on the sides of the airframe might flow into the engine in the laminar condition due to short distance from the side edge to the engine.[21] To make the layer turbulent, the airframe configuration of the model A will be favorable to the engine.

SSTO Thermal Condition

Inside thermal environment in orbit

The combined cycle engine will be used to the SSTO plane. The SSTO plane goes to space after aerodynamic heating during flight. The Thermal Protection System (TPS) tile is heated. The space is in the vacuum condition. The TPS tile will be insulated thermally by the vacuum condition. The heat in the tile will be conducted into the inside of the plane. Inside the plane, there are payload, crews, and cryogenic propellant tanks. The inside thermal environment in the orbit is a key issue of the SSTO plane.

Figure 23 shows history of the TPS tile temperatures in the ascending flight and in the orbit.[22] The maximum inside temperature appeared after arrival to the orbit. The temperature can be suppressed with increase of the thickness of the tile. Figure 24 shows the maximum temperature during the flight against the flight dynamic pressure. The maximum outside temperature of the tile decreased with decrease of the flight dynamic pressure. The maximum inside temperature, however, increased with decrease of the flight dynamic pressure. It was caused by increase of the flight time, the period of aerodynamic heating. High flight dynamic pressure is favorable to suppress the inside temperature of the TPS tile.

Thermal protection in descending entry flight

Another problem is cooling of the leading edge of the SSTO plane airframe. The SSTO plane flies in hypersonic speed in the air. To reduce drag and to increase thrust of the engine, the leading edge of the plane should be sharp and it will be cooled actively. The problem is cooling of the sharp leading edge of the airframe during the descending entry flight.

Coolant amount of the leading edge was calculated with the flight simulation of the SSTO plane.[23] Figure 25 shows the amount of the hydrogen coolant of the leading edge. The amount was several percents of the hydrogen consumed in the ascending flight. The leading edge of the airframe could be cooled. Figure 26 shows history of the tile temperature in the descending flight. The flight time was about three times as long as the time of ascending flight. The long flight time was due to small mass and large volume of the SSTO plane. The tile temperature on the outside surface was lower than the limit temperature of the tile. The maximum tile temperature on the inside surface appeared after landing. The required thickness of the tile was larger than the thickness in the ascending flight. It was due to the longer flight time.

Summary

Recent results of the conceptual studies on the combined-cycle engine and the SSTO plane are presented. Results of the experimental component tests are also presented. Through the investigations, possibilities of the combined-cycle engine and the aerospace plane are now being made clear.

Acknowledgements

The author thanks members of the engine system team for preparing, discussing and editing this manuscript.

References

1) Escher, W. J. D.: A U.S. History of Airbreathing/Rocket Combined-Cycle (RBCC) Propulsion for Powering Future Aerospace Transports, with a Look ahead to the Year 2020, 14th International Symposium on Air Breathing Engines Paper. ISABE 99-7028, Sep. 1999.

2) Olds, J. R., and Bradford, J. E.: SCCREAM: A Conceptual Rocket-Based Combined-Cycle Engine Performance Analysis Tool, *Journal of Propulsion and Power*, Vol. 17, No. 2, 2001, pp. 333-339.

3) Heiser, W. H., Pratt, D. T., Daley, D. H., and Mehta, U. B.: Hypersonic Airbreathing Propulsion. AIAA Education Series, AIAA, Washington, DC, 1994, pp. 447-451.

4) Siebenhaar, A.: Strutjet Evolves to Meet Air-Breathing Propulsion Challenges for the 21st Century, 13th International Symposium on Air-Breathing Engines, Paper 97-7135, Sep. 1997.

5) Bertin, J. J.: Hypersonic Aerothermodynamics, AIAA Education Series, AIAA, Washington, DC, 1994, pp. 592-594.

6) Chinzei, N., Masuya, G., Kudo, K., Murakami, A., and Komuro, T.: Experiment on Multiple Fuel Supplies to Air Breathing Rocket Combustors, *Journal of Propulsion and Power*, Vol. 4, No. 1, 1987, pp. 26-32.

7) Kanda, T., and Kudo, K.: Cooling Requirement of Combined-Cycle Engine in Descending Flight, to be presented at 24th *International Symposium on Space Technology and Science*, Japan, May 2004.

8) Kanda, T., and Kudo, K.: Conceptual Study of a Combined-Cycle Engine for an Aerospace Plane. *Journal of Propulsion and Power*, Vol. 19, No. 5, 2003, pp. 859-867.

9) Kanda, T., Masuya, G., and Wakamatsu, Y.: Propellant Feed System of a Regeneratively Cooled Scramjet, *Journal of Propulsion and Power*, Vol. 7, No. 2, 1991, pp. 299-301.

10) Tani, K., Kanda, T., and Tokunaga, T.: Starting Characteristics of Scramjet Inlets, *Proceedings of 11th International Symposium on Air-Breathing Engines*, Vol. 2, AIAA, Washington, DC, 1993, pp. 1071-1080.

11) Kanda, T., Hiraiwa, T., Izumikawa, M., and Mitani, T.: Experimental Evaluation for Mass Capture Ratio of Scramjet Inlets, *Journal of Propulsion and Power*, to be appeared.

12) Kubota, S., Tani, K., and Masuya, G.: Aerodynamic Performances of Combined-Cycle Inlet, to be presented at 24th International Council of the Aeronautical Sciences, Aug. 2004.

13) Tani, K., Kanda, T., Kudo, K., and Akihisa, D.: Effect of Sides-Spillage from Airframe on Scramjet Engine Performance, *Journal of Propulsion and Power*, Vol. 17, No. 1, 2001, pp. 139-145.

14) Akihisa, D., Kanda, T., Tani, K., Kudo, K., and Masuya, G.: Effect of Integration of Scramjet into Airframe on Engine Performance and Payload, *Journal of Propulsion and Power*, Vol. 18, No. 5, 2002, pp. 1026-1032.

15) Aoki, S., Lee, J., Masuya, G., Kanda, T., Kudo, K., and Murakami, A.: Experimental Investigation of an Ejector-jet, AIAA Paper 2003-0188, Jan.

2003.
16) Kanda, T., Chinzei, N., Kudo, K., and Murakami, A.: Dual-mode Operation in a Scramjet Combustor, to be appeared in *Journal of Propulsion and Power*.
17) Kato, K., Kanda, T., Kudo, K., and Murakami, A.: Ramjet-mode Operation in a Scramjet Combustor, 16h International Symposium on Air-Breathing Engines Paper, ISABE 2003-1150, Sep. 2003.
18) Kanda, T., Kudo, K., Kato, K., and Murakami, A.: Scramjet mode tests of a Combined-Cycle Engine Combustor, AIAA Paper 2003-7051, Dec. 2003.
19) Kodera, M., Kanda, T., and Tani, K.: Effect of Airframe Geometry on Thrust Performance of Aerospace Plane, AIAA Paper 2000-3342, Jul. 2000.
20) Kanda, T., Kato, K., Kodera, M., Kudo, K., and Murakami, A.: Effect of Airframe Configuration on Airflow Condition to Engine in Hypersonic Flow, AIAA Paper 2003-3420, Jun. 2003.
21) Private communication with Dr. Shinji Nagai, Senior Researcher of Japan Aerospace Exploration Agency.
22) Kanda, K, and Kudo, K.: Preliminary Study of Thermal Protection System of a Single-Stage-to-Orbit Plane, *Proceedings of the 22nd International Symposium on Space Technology and Science*, the Japan Society for Aeronautical and Space Sciences, Tokyo, Japan, May 2000, pp. 1354-1360.
23) Kudo, K., and Kanda, T.: Preliminary Study of Thermal Protection System of a Single-Stage-to-Orbit Plane (II), *Proceedings of the 23rd International Symposium on Space Technology and Science*, the Japan Society for Aeronautical and Space Sciences, Tokyo, Japan, 2002, pp. 1075-1080.